Journal of Electronics, Electromedical Engineering, and Medical Informatics
Homepage: jeeemi.org; Vol. 8, No. 2, April 2026, pp: 806-824 e-ISSN: 2656-8632

RESEARCH ARTICLE OPEN ACCESS

A Hybrid Quantum-Inspired Deep Learning Framework with Bio-Inspired Optimization for Cardiovascular Disease Prediction

Vinoth Rathinam[1], Valarmathi K[1], Madhumathi A[1] and Lalitha S.D[2]

[1] Department of Electronics and Communication Engineering, P.S.R. Engineering College, Tamilnadu, India.
[2] Department of Computer Science and Engineering, R.M.K. Engineering College, Chennai, India.

Corresponding author: Vinoth Rathinam. (e-mail: vinoth@psr.edu.in), **Author(s) Email**: Valarmathi K. (e-mail: valarmathi@psr.edu.in), Madhumathi A. (e-mail: mm3878788@gmail.com), Lalitha S.D. (e-mail: sdl.cse@rmkec.ac.in)

Abstract **The prognostication of cardiovascular diseases is paramount for the facilitation of early detection and enhancement of patient prognoses. It introduced a novel hybrid deep learning architecture that amalgamates Convolutional Neural Networks (CNN), Quantum Convolutional Neural Networks (Q-CNN), Long Short-Term Memory (LSTM) networks, Quantum-Inspired Long Short-Term Memory (Q-LSTM) models, Denoising Autoencoders (DAE), and Transformer Encoder–Decoder frameworks. The quantum models were innovatively structured by integrating unitary transformations and Hilbert space representations within traditional deep learning paradigms. Hyperparameter optimization, including learning rate, hidden unit count, dropout rates, and batch size, was executed utilizing the Greylag Goose Optimization (GGO) algorithm, which was meticulously chosen after initial benchmarking against conventional optimization techniques. These models underwent training and validation processes on a meticulously curated clinical dataset encompassing both demographic and clinical attributes, with preprocessing measures implemented to rectify missing data and address class imbalances. Among the array of assessed models, the GGO-optimized Q-LSTM exhibited superior performance, attaining an accuracy of 98.05% (95% CI: 96.8–99.2%), a precision of 1.00, a recall of 98.96%, an F1-score of 97.95%, and an AUC-ROC of 0.980. The DAE demonstrated an accuracy of 97.08% alongside an AUC-ROC of 0.989. Future research endeavors will focus on external validation and statistical significance testing to evaluate model generalization. Additionally, considerations regarding model interpretability through SHAP analysis and the practical deployment aspects (e.g., integration with Electronic Health Records) are thoroughly examined. This investigation underscores the assertion that the integration of deep learning methodologies, quantum-inspired modeling, and bio-inspired optimization strategies can markedly enhance predictive analytics for cardiovascular disease identification, while concurrently underscoring the critical importance of model interpretability and rigorous validation.**

Keywords **Cardiovascular disease, Quantum CNN, Quantum LSTM, Transformer, Autoencoder, Grey-lag Goose Optimization, Ensemble Learning**.

I. Introduction

Cardiovascular disease (CVD) continues to represent the foremost cause of mortality on a global scale, resulting in an alarming estimate of approximately 18 million deaths each year, as reported by the World Health Organization in the year 2023. The implementation of early detection methodologies and the precision of risk prediction models are paramount in the endeavor to diminish mortality rates while simultaneously optimizing healthcare interventions across various clinical settings [1]. However, it is important to acknowledge that the current diagnostic techniques available are frequently hindered by the intrinsic complexity, variability, and inherent noise that characterize clinical data, which complicates the diagnostic process [2-4]. In recent years, machine learning (ML) and deep learning (DL) strategies have exhibited substantial promise in enhancing predictive modeling capabilities within the healthcare domain. Nevertheless, it is crucial to note that traditional ML and DL models, including but not limited to logistic regression, decision trees, convolutional neural networks (CNNs), and recurrent neural networks (RNNs), confront significant challenges when tasked with processing noisy, high-dimensional, and temporally dynamic datasets that are often encountered in medical contexts [5-7]. Among these challenges, one can identify the difficulty of managing

Manuscript received 30 Dec 2025; Revised 10 Feb 2026; Accepted 20 April 2026; Available online 30 April 2026
Digital Object Identifier (**DOI**): https://doi.org/10.35882/jeeemi.v8i2.1440

long-range dependencies and complex feature interactions that are vital for accurate predictions.

Moreover, they are defined as being very sensitive to missing values of data and outliers that may exist in the data, hence giving a biased result and invalid predictions. Moreover, it is also accompanied by a low capacity of these classical approaches to describe complex non-linear relationships present in healthcare data in an efficient way [8]. In addition to that, the issue of generalization in multiple patient groups can severely threaten both the applicability of such predictive models to a more realistic clinical scenario. While fully eliminating or at least partly reducing these severe limitations, we would propose the development of a groundbreaking hybrid deep learning model that would naturally apply all the convolutions to the quantum Hilbert spaces, therefore, allowing even more successful recognition of the spatial features of structured clinical data, which is a significantly important step towards the appropriate level of risk assessment. The Quantum LSTMs, on the other hand, utilize quantum memory units and superposition ideas in intelligent learning of complex sequential dependencies, which enhances the performance and loss of information that can otherwise overpower the intentions of the sequential prediction of the model. The key strengths of these realistic quantum systems for several medical tasks, including: first, they enhance feature representation, encourage noise resistance, and also enhance the rate of convergence, which are critical components needed in the development of clinical quality prediction systems that have a stable capability to predict cardiovascular events.

The suggested hybrid architecture combines a number of supplementary learning units into one processing pipeline. The Denoising Autoencoder (DAE) is first used to carry out noise reduction and latent features extraction of the clinical data. The extracted features in refined forms are then fed to the Q-CNN to extract spatial patterns, and the Q-LSTM to model sequential relationships between cardiovascular features. Simultaneously, the Transformer Encoder Decoder models feature interactions of features globally via self-attention. These models are optimized using the Greylag Goose Optimization (GGO) algorithm, which optimizes the hyperparameters to produce an optimal predictive configuration. These modules also interact with each other as the proposed framework architecture (Fig. 1) demonstrates. In this paper, quantum-inspired denotes the application of mathematical concepts based on quantum mechanics to classical deep learning models and not the deployment of real quantum computing. In particular, both the Q-CNN and Q-LSTM models feature unitary-like transformations and representation of features in Hilbert space to represent superposition-like feature interactions in a manner that is norm stable. Such mechanisms increase the expressiveness of the features, as well as permit the models to model nonlinear relationships between cardiovascular risk factors in more detail than standard architectures.

II. Related Work

Recent progress in the domain of computational healthcare has significantly highlighted the pressing necessity for sophisticated models that possess the capability to autonomously acquire and learn intricate hierarchical structures, non-linear relationships, and temporally sensitive features derived from a wide array of medical data sources that are both diverse and multifaceted [9]. In particular, the multimodal nature of electronic health records (EHRs) that incorporates different types of data, such as structured variables, time series vital signs, diagnostic imaging, and narrative clinical notes, requires the creation of predictive systems that are capable of executing adaptive reasoning across multiple positions, thus increasing the efficiency of clinical decision-making processes. Traditional deep learning systems, despite their significant capabilities and usefulness, often require a high level of manual feature engineering, manual hyperparameter optimization, as well as the availability of large and labeled datasets, to achieve a level of performance that may be considered reliable and trustworthy [10]. Nevertheless, in very many clinical settings, the achievement of these preconditions can become extremely difficult, mainly because of such limitations as the lack of data and the heterogeneity of patient groups, as well as because of the plethora of ethical issues that complicate the process of data gathering and application.

Bukhari et al. [11] introduced a hybrid model of SCNN LFGOA based on predicting cardiovascular diseases and emphasized the use of convolutional networks and bio-inspired optimization approaches. To improve the performance of feature selection and prediction in cardiovascular datasets, Shanshan Wang et al. [12] used Pearson Correlation, ensemble, and Principal Component Analysis techniques. To deal with the problem of class imbalance and missing values in the Framingham Heart Study dataset, Omotehinwa et al. [13] used LightGBM in conjunction with Bayesian Optimization, MICE imputation, and Borderline SMOTE. Haifeng Zhang et al. [14] investigated nature-inspired methods of optimization algorithms, such as Slime Mold and Pathfinder optimization, with XGBoost classifiers to enhance the prediction of heart disease. Mohammed Amine Bouqentar et al. [15] comparatively implemented the classical machine learning algorithms, which include Random Forest, SVM, Decision Tree, and Logistic Regression, on the Cleveland heart dataset and evaluated the efficacy of various classifiers on clinical prediction. B. This work

Manuscript received 30 Dec 2025; Revised 10 Feb 2026; Accepted 20 April 2026; Available online 30 April 2026
Digital Object Identifier (**DOI**): https://doi.org/10.35882/jeeemi.v8i2.1440

was based on the use of an Optimal Scrutiny Boosted Graph Convolutional LSTM model combined with the Eurygaster Optimization Algorithm [16] with a sequence pattern recognition objective in cardiovascular and diabetes data. Tahseen Ullah et al. [17] optimized ensemble models such as Random Forest and Extra Tree using Particle Swarm Optimization across both small and large heart disease datasets.

Subbulakshmi Pasupathi et al. [18] have used the Hybrid Harris Hawks Optimization (H-HGO) framework to increase the predictive potential of the Random Forest models by embedding context-based features. Tariq Mahmood et al. [19] assessed the state-of-the-art machine learning models using Boosted Decision Trees and proved that ensemble methods are effective in terms of the classification of heart diseases. J. To enhance interpretability and high performance of the model on large cardiovascular datasets, Jasmine Gabriel et al. [20] designed a dual tier ANOVA Chi-Squared feature selection (AnoX2) framework. D. Yaso Omkari et al. [21] introduced the Two-Layer Voting (TLV) model that involves a combination of hard and soft voting to select features, which boosts the predicates of the most datasets. Besides, Tariq Mahmood et al. [22] implemented XGBoost with methodical feature selection on CHD datasets to perform optimal prediction pipelines. The usefulness of hybridization and feature engineering in the context of hybrid ACVD-HBOMDL framework was proposed by Marwa Obayya et al. [23] on a range of datasets. J. Jasmine Gabriel et al. [24] came up with the BSOXGB framework through incorporating features selection (BorutaShap) with hyperparameter optimization (Optuna) to enhance interpretability and predictive power. Pendela Kanchanamala et al. [25] examined the optimization methods to cardiovascular data in order to maximize a classifier. Neeraj Sharma et al. [26] used hybrid deep learning architecture, which incorporates BiLSTM and GRU units to analyze sequential clinical data. Manikandan R et al. [27] enhanced Two-fold clustering with LSTM for predictive modeling using electronic health records. Mert Ozcan et al. [28] utilized the CART algorithm to classify cardiovascular disease cases, while R. Valarmathi et al. [29] applied ensemble learning strategies on the Cleveland dataset to improve prediction reliability.

Although significant progress in the use of machine learning and deep learning methods to predict cardiovascular diseases, there are still some limitations. Existing strategies primarily emphasize either feature selection, classical neural networks or optimization-based models in isolation, and therefore lack the capacity to jointly model nonlinear clinical relations, temporal correlations between clinical variables and resistance to noisy medical data. Also, traditional models can be based on outdated feature representations and can be ineffective in learning more complex interactions between heterogeneous cardiovascular risk factors. In order to overcome these shortcomings, the proposed hybrid quantum-based deep learning architecture will combine denoising feature learning in a Denoising AutoEncoder, spatial patterns extraction in a Q-CNN and temporal dependencies modeling in a Q-LSTM, with a Transformer module that reflects the global feature correlation through attention processes. The Greylag Goose Optimization algorithm also optimizes hyperparameters in these components in an adaptive manner and hence offers a more powerful and high-capacity predictive architecture in detecting cardiovascular diseases.

III. Method

The proposed Hybrid Quantum-Inspired Deep Learning Framework with Bio Inspired Optimization is designed to enhance the accuracy, interpretability, and robustness of cardiovascular disease prediction from complex and high-dimensional medical data. The framework integrates three key paradigms quantum inspired neural computation, bio inspired hyperparameter optimization, and noise resilient feature learning into a cohesive predictive model that simulates quantum parallelism while maintaining classical computational feasibility as shown in Fig. 1. The basic idea behind the framework is to integrate Quantum Convolutional Neural Networks (Q-CNN) and Quantum Long Short-Term Memory (Q-LSTM): the architecture should address both spatial and temporal correlations that can be found in cardiovascular data. Learning of the complex structural and morphological features of clinical or physiological signals is carried out by the Q-CNN component, which uses the quantum convolution operations to encode the information into amplitude states. These processes allow pattern recognition of multi-dimensional data efficiently, and a simulation of the principle of entanglement and superposition of quantum computing. Simultaneously, Q-LSTM module captures sequential dependencies and time-oriented patterns of progression of variations in patient health, where continuity in time and physiological patterns are effectively captured in the latent space.

In order to develop the most optimal configurations and convergence, the framework relies on Greylag Goose Optimizer (GGO) bio inspired metaheuristic algorithm that the framework relies on to recreate the process of migration of the geese when creating a flock. The GGO algorithm is a dynamic fine-tuning of the significant hyperparameters of the Q-LSTM and Q-CNN models, such as the learning rate, the dropout ratio, and the memory cell size, to achieve the lowest

Manuscript received 30 Dec 2025; Revised 10 Feb 2026; Accepted 20 April 2026; Available online 30 April 2026
Digital Object Identifier (**DOI**): https://doi.org/10.35882/jeeemi.v8i2.1440

loss on validation and the highest predictive accuracy. Such an optimization process offers an effective trade-off of exploration and exploitation, leading to faster convergence and reduced overfitting. In addition, a Denoising Autoencoder (DAE) module is also introduced as a representation learning sub-block and preprocessing module to make the framework more robust to data imperfections and noise, which is a frequent issue with clinical datasets. Salient and stable latent features are determined by the DAE by reconstructing original signals using noisy inputs, which makes the subsequent layers of quantum-inspired learning robust. The pipeline operates in the following way: any cardiovascular dataset of input is preprocessed and transmitted to the DAE to be refined and denoised in features. The representations of the clean features are then fed into the Q-CNN to learn spatial features, and then the Q-LSTM to learn time. The GGO algorithm finds the best possible setup of the hyperparameters of the whole network by optimizing the hyperparameters dynamically. Finally, the hybrid model produces a correct cardiovascular disease predictor outcome. This kind of synergetic integration of the quantum-inspired computation, bio-inspired optimization, and noise-insensitive learning shapes a powerful and universalistic predictive model that can be applied in the medical decision support systems of the real world.

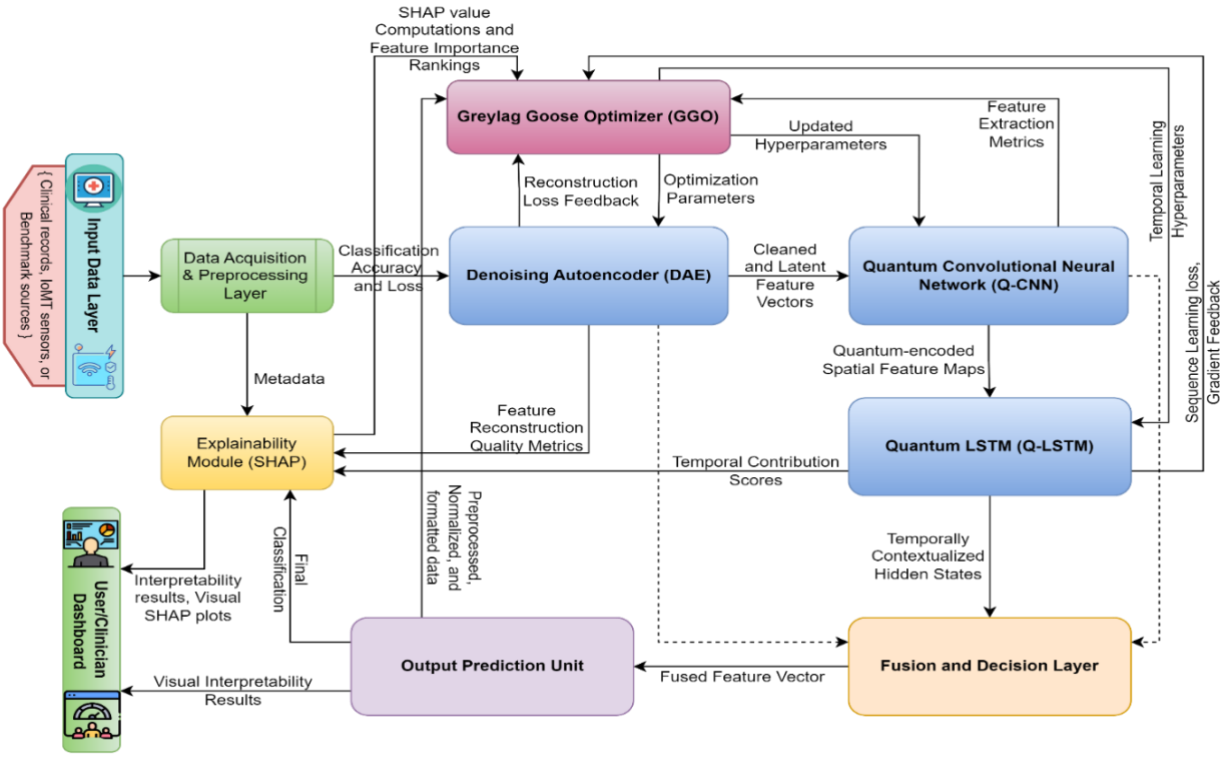

Fig. 1. Proposed Hybrid Quantum Inspired Framework

A. Data Acquisition and Preprocessing

The data acquisition and preprocessing stage forms the foundation of the proposed Hybrid Quantum-Inspired Deep Learning Framework, ensuring data integrity, quality, and readiness for quantum-enhanced learning [30]. This stage encompasses structured data collection, cleaning, normalization, encoding, and segmentation to preserve both spatial and temporal characteristics crucial for cardiovascular disease (CVD) prediction.

1. Dataset Description

The dataset utilized in this study comprises electronic health records (EHRs) and clinical measurements of cardiac patients, including physiological signals, demographic variables, and diagnostic indicators, as shown in Table 1. Each instance is represented as a multidimensional vector as defined in Eq. (1) as follows [2], where $\boldsymbol{x_i} \in \mathbb{R}^{\boldsymbol{n}}$ denotes the feature vector containing n patient attributes, and $\boldsymbol{y_i} \in \{\boldsymbol{0}, \boldsymbol{1}\}$ indicates the disease status (1 = Disease, 0 = No Disease). The entire dataset D_{total} is partitioned into training, validation, and testing subsets as defined in Eq. (2) as follows [8]. Typically, an 80–10–10 split ratio is employed to ensure adequate model generalization and unbiased evaluation.

$$D = \{x_i, y_i\}_{i=1}^{N} \quad (1)$$

$$D_{total} = D_{train} \cup D_{val} \cup D_{test}, \quad D_{train} \cap D_{val} \cap D_{test} = \emptyset \quad (2)$$

Manuscript received 30 Dec 2025; Revised 10 Feb 2026; Accepted 20 April 2026; Available online 30 April 2026
Digital Object Identifier (**DOI**): https://doi.org/10.35882/jeeemi.v8i2.1440

2. Data Cleaning and Normalization

Data preprocessing begins with the elimination of incomplete or inconsistent records, followed by imputation of missing values using a median-based strategy to preserve statistical stability.

$$x' = \frac{x - x_{min}}{x_{max} - x_{min}} \quad (3)$$

Continuous features such as cholesterol level, resting blood pressure, and maximum heart rate are normalized using min–max scaling as defined in Eq. (3) as follows [2]. This normalization confines all feature values within the range [0,1], ensuring uniform gradient propagation during model training.

3. Encoding and Feature Structuring

Categorical features (e.g., sex, chest pain type, exercise-induced angina) are transformed via one-hot encoding, converting nominal attributes into binary vectors. Each encoded feature is concatenated with numerical attributes to form a unified input vector x_i. The resultant structured data is reshaped into tensor form, suitable for convolutional and sequential processing by the Q-CNN and Q-LSTM layers. To align with the spatial encoding process required for quantum feature mapping, each record is converted into a pixel-mapped representation, where each attribute corresponds to a pixel intensity. Thus, clinical variables are spatially encoded as grayscale images, allowing the Q-CNN to extract localized feature correlations that would otherwise be inaccessible through traditional tabular learning.

Table 1. Description of Heart Disease Dataset

Feature	Description	Type	Range / Values
Age	Age of the patient	Numeric	29 – 77
Sex	Sex (1 = male; 0 = female)	Binary	0, 1
Cp	Chest pain type	Categorical	0, 1, 2, 3
trestbps	Resting blood pressure (mm Hg)	Numeric	94 – 200
Chol	Serum cholesterol (mg/dl)	Numeric	126 – 564
Fbs	Fasting blood sugar ¿ 120 mg/dl (1 = true)	Binary	0, 1
restecg	Resting ECG results	Categorical	0, 1, 2
thalach	Maximum heart rate achieved	Numeric	71 – 202
Exang	Exercise-induced angina (1 = yes)	Binary	0, 1
oldpeak	ST depression induced by exercise	Numeric	0.0 – 6.2
Slope	Slope of peak exercise ST segment	Categorical	0, 1, 2
Ca	Number of major vessels colored	Numeric	0 – 3
Thal	Thalassemia (3 = normal; 6 = fixed defect)	Categorical	0, 1, 2, 3, 6, 7
Target	Heart disease (1 = yes, 0 = no)	Binary	0, 1

4. Noise Injection and Augmentation

Given the inherent variability in clinical datasets, noise-injection techniques are incorporated to enhance the model's resilience to real-world imperfections. Gaussian noise $\mathcal{N}(0, \sigma^2)$ is added to selected input features during training to simulate sensor or measurement noise as defined in Eq. (4) as follows [31]. These augmented samples are subsequently processed by the Denoising Autoencoder (DAE), which reconstructs clean latent representations. This process improves the stability of feature extraction and minimizes overfitting by regularizing the learned feature space.

$$x_{noisy} = x + \epsilon, \epsilon \sim \mathcal{N}(0, \sigma^2) \quad (4)$$

This preprocessing pipeline ensures that the input data is balanced, denoised, and structurally consistent with the hybrid quantum-inspired architecture. The combination of feature normalization, spatial encoding, and noise-resistant representation learning significantly enhances the robustness of the downstream predictive modeling process.

B. Quantum Convolutional Neural Network (Q-CNN) Architecture

The Quantum Convolutional Neural Network (Q-CNN) represents the first stage of the proposed hybrid framework, designed to extract highly discriminative spatial features from clinical data transformed into quantum encoded tensors. By leveraging the principles of quantum superposition and entanglement, the Q-CNN enables parallel processing of multidimensional patterns, enhancing feature expressivity and computational efficiency compared to its classical counterpart [31]. The preprocessed clinical data D_{pre} is transformed into quantum states through an amplitude encoding scheme, where each normalized feature vector $x_i = [x_1, x_2, \ldots, x_n]$ is mapped onto a quantum state $|\psi_i\rangle$ as defined in Eq. (5) as follows [4]. This encoding ensures that all features are simultaneously represented within a high-dimensional Hilbert space, allowing the quantum circuit to capture correlations that are nonlinearly separable in classical space.

Manuscript received 30 Dec 2025; Revised 10 Feb 2026; Accepted 20 April 2026; Available online 30 April 2026
Digital Object Identifier (**DOI**): https://doi.org/10.35882/jeeemi.v8i2.1440

$$|\psi_i\rangle = \sum_{j=1}^{n} x_j |j\rangle, \text{ such that } \sum_{j=1}^{n} |x_j|^2 = 1 \quad (5)$$

1. Quantum Convolution Operation

The quantum convolution layer applies parameterized unitary transformations to these encoded quantum states, mimicking the convolution process of a classical CNN but operating in a probabilistic amplitude domain, as shown in Fig. 2. The transformation can be represented as defined in Eq. (6) as follows [9]. Here, U_{conv} is the quantum convolution operator, $f(\alpha_i)$ denotes the learnable filter coefficients represented as rotation angles in the quantum gates, and $|i\rangle$ indicates the computational basis states. This operation extracts spatially entangled feature maps by exploiting the interactions between qubits through controlled rotation and entanglement gates (e.g., CNOT and CRZ). These interactions enhance the representation power of the network, enabling efficient identification of subtle clinical variations that signify early cardiovascular anomalies.

$$U_{conv}|\psi\rangle = \sum_{i} f(\alpha_i)|i\rangle \quad (6)$$

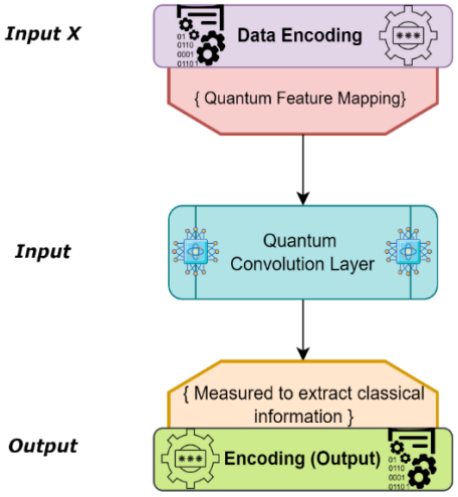

Fig. 2. Quantum Convolution Architecture

2. Quantum Pooling and Measurement

Following convolution, quantum pooling is performed to reduce the dimensionality of the feature space while preserving essential characteristics. Quantum pooling is achieved through a partial measurement strategy, wherein a subset of qubits is measured to collapse their probability amplitudes. where M_P denotes the measurement operator applied to selected qubits. This pooling operation introduces stochastic regularization, mitigating overfitting by randomly collapsing certain state amplitudes, similar to dropout in classical CNNs. The measurement outcomes correspond to observable feature representations, which are further processed by classical layers for interpretation and integration with the Quantum-LSTM stage. The Greylag Goose Optimization (GGO) algorithm fine-tunes the Q-CNN parameters, such as rotation angles, layer depth, and kernel size, to enhance predictive performance. The optimization process follows the dynamics of cooperative swarm behavior, as outlined in algorithm 1 below.

$$|\psi_{pooled}\rangle = M_P(U_{conv}|\psi\rangle) \quad (7)$$

ALGORITHM 1: GGO-BASED OPTIMIZATION FOR Q-CNN

***Input**: Quantum-CNN architecture with initial parameters Θ*
***Output**: Optimized parameter configuration Θ_{best}*

1. Initialize GGO population with candidate Q-CNN parameter sets
2. ***While*** convergence criterion not met ***do***
3. ***for*** each goose in the population ***do***
4. Train Q-CNN using assigned parameter set
   Evaluate fitness based on validation accuracy
   Update position using GGO movement dynamics
5. ***End for***
   Update global and personal best positions
6. ***End while***
7. ***Return*** Θ_{best}

Prior to selecting the Greylag Goose Optimization (GGO) algorithm, a pre-test benchmarking of the algorithm was performed against the common optimization strategies, such as Random search and gradient-based Adam algorithm, to tune the hyperparameters. Comparison was conducted based on validation accuracy, convergence behavior and stability with respect to training epoch as measures. The findings demonstrated that GGO offered a superior exploration versus exploitation tradeoff, which allowed for more stable discovery of optimal hyperparameter settings and better convergence stability. Resting on these observations, GGO was chosen as the common optimization approach to the suggested hybrid framework. The GGO ensures a balanced trade-off between exploration (searching diverse parameter regions) and exploitation (refining near-optimal configurations), enabling rapid convergence toward the most effective Q-CNN setup as defined in Eq. (7) as follows [8].

Manuscript received 30 Dec 2025; Revised 10 Feb 2026; Accepted 20 April 2026; Available online 30 April 2026
Digital Object Identifier (**DOI**): https://doi.org/10.35882/jeeemi.v8i2.1440

C. Quantum Long Short-Term Memory (Q-LSTM) Architecture

The Quantum Long Short-Term Memory (Q-LSTM) architecture extends the classical LSTM model by embedding quantum-inspired transformations within its recurrent and gating mechanisms, as shown in Fig. 3. This integration enables the model to preserve temporal dependencies more effectively while maintaining stability and reduced gradient dissipation during sequential learning. In cardiovascular disease prediction, temporal relationships among diagnostic features—such as blood pressure variability, heart rate trends, and lipid profile evolution are critical for accurate prognosis. The Q-LSTM captures these dependencies by leveraging quantum coherence and unitary operations, ensuring norm preservation throughout state transitions.

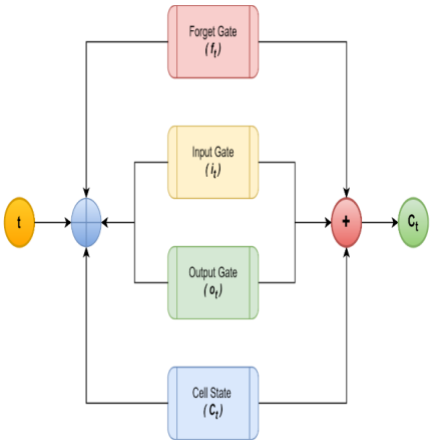

Fig. 3. Quantum LSTM Architecture

1. Quantum Gate Operations and State Representation

Each time step t as defined in Eq. (8) as follows [2], receives input $X_t$and previous hidden state h_{t-1}, which are processed through quantum-inspired gate operations that emulate the behavior of LSTM memory mechanisms. The conventional LSTM equations are extended using unitary transformations $U(\cdot)$ to maintain state normalization as defined in Eq. (9) to Eq. (13) as follows [4]:

Forget Gate:

$$f_t = \sigma\left(W_f X_t + U_f h_{t-1} + b_f\right) \quad (8)$$

Input Gate:

$$i_t = \sigma(W_i X_t + U_i h_{t-1} + b_i) \quad (9)$$

Candidate Cell State (with Unitary Transformation):

$$\tilde{C}_t = \tanh\left(U(W_c X_t + U_c h_{t-1} + b_c)\right) \quad (10)$$

Cell State Update:

$$C_t = f_t \odot C_{t-1} + i_t \odot \tilde{C}_t \quad (11)$$

Output Gate and Hidden State:

$$o_t = \sigma(W_o X_t + U_o h_{t-1} + b_o) \quad (12)$$

$$h_t = o_t \odot \tanh(C_t) \quad (13)$$

Here, $\odot$ represents element-wise multiplication, and the unitary normalization $U(z) = \frac{z}{\|z\|}$ ensures that the magnitude of the quantum-inspired transformations remains bounded, preserving quantum-like stability across recurrent operations.

2. Quantum Memory Encoding

In this framework, as defined in Eq. (14) as follows [32], each cell state C_t and hidden state $h_t$are encoded as quantum amplitude vectors. These are treated as pure states $|\psi_t\rangle$ in the quantum Hilbert space, where temporal evolution follows:

$$C_t = U_{cell} |\psi_t\rangle, i_t = U_{input} |\psi_t\rangle, f_t = U_{forget} |\psi_{t-1}\rangle \quad (14)$$

This encoding ensures that the model retains long-term dependencies without degradation, as the unitary operations prevent information loss through norm-preserving transformations. Consequently, the Q-LSTM achieves enhanced memory retention, which is particularly beneficial when analyzing long-term cardiac patient records. The Q-LSTM exploits quantum parallelism to process multiple temporal patterns concurrently. Through controlled unitary operations, different hidden states interact coherently, analogous to quantum entanglement, facilitating deeper cross-temporal correlations. This property enables the network to uncover subtle time-based clinical variations that may be undetectable by purely classical models. The training process of Q-LSTM is optimized using the Greylag Goose Optimization (GGO) algorithm. The GGO enhances convergence by balancing exploration (diversity of candidate solutions) and exploitation (fine-tuning near-optimal hyperparameters), which is crucial for optimizing parameters such as memory size, learning rate, and dropout ratio.

It is necessary to mention that the suggested architecture is quantum-motivated and executed on a classical computing platform. The quantum-inspired behavior is modeled by the mathematical structures based on quantum mechanics instead of physical quantum gates. Specifically, feature vectors are regarded as state representations in a Hilbert space, and the transformation $U(\cdot)$ is a unitary-inspired normalization that maintains feature, vectors norms, and balances out the propagation of features between layers. In the QCNN architecture, the transformation is used following convolution operations to simulate quantum state evolution. Equally, the QLSTM is based on the same transformation as its candidate memory state update, allowing stable state transitions between succeeding time steps that are similar to unitary quantum transformations during temporal modeling. The optimization process follows GGO-Based Optimization for Q-LSTM and DAE, as outlined in algorithm 2 and algorithm 3 below.

Manuscript received 30 Dec 2025; Revised 10 Feb 2026; Accepted 20 April 2026; Available online 30 April 2026
Digital Object Identifier (**DOI**): https://doi.org/10.35882/jeeemi.v8i2.1440

ALGORITHM 2: GGO-BASED OPTIMIZATION FOR Q-LSTM

***Input**: Q-LSTM architecture and initial hyperparameters*
***Output**: Optimized Q-LSTM parameter configuration* Θ_{best}

1. Initialize GGO population with Q-LSTM hyperparameter sets
2. ***While*** convergence not achieved ***do***
3. ***for*** each goose in the population ***do***
4. Train Q-LSTM using assigned hyperparameters
   Compute fitness based on validation loss or accuracy
   Update position and velocity using GGO dynamics
5. ***End for***
   Update global and personal best positions
6. ***End while***
7. ***Return*** Θ_{best}

D. Denoising Autoencoder (DAE)

The Denoising Autoencoder (DAE) plays a critical role in the proposed hybrid framework by learning noise-invariant and robust feature representations from potentially noisy or incomplete clinical data. Clinical datasets often suffer from measurement errors, sensor variability, or missing entries, which can degrade the performance of deep learning models, as shown in Fig. 4. The DAE mitigates these issues by reconstructing clean input features from deliberately corrupted data, ensuring that downstream Quantum-CNN and Q-LSTM models receive high-quality latent embeddings. During training, Gaussian noise is added to the input features to simulate real-world clinical data perturbations as defined in Eq. (15) as follows [4]. Where X_i is the original input, $\tilde{X}_i$is the noisy input, ϵrepresents Gaussian noise, and $I$is the identity matrix. This process encourages the encoder to focus on salient, stable patterns, promoting robustness and generalization.

$$\widetilde{\boldsymbol{X}}_{\boldsymbol{i}} = \boldsymbol{X}_{\boldsymbol{i}} + \boldsymbol{\epsilon}, \boldsymbol{\epsilon} \sim \boldsymbol{\mathcal{N}}(\boldsymbol{0}, \boldsymbol{\sigma}^{\boldsymbol{2}}\boldsymbol{I}) \quad (\mathbf{15})$$

The DAE comprises two main components:
Encoder: Maps the corrupted input $\widetilde{\boldsymbol{X}}_{\boldsymbol{i}}$ to a lower-dimensional latent representation $\boldsymbol{z}_{\boldsymbol{i}}$ as defined in Eq. (16) as follows [31]. where $\boldsymbol{W}_{\boldsymbol{e}}$ and $\boldsymbol{b}_{\boldsymbol{e}}$ are learnable encoder weights and biases, and $\boldsymbol{\sigma}(\cdot)$ is an activation function (ReLU or Sigmoid).

$$\boldsymbol{z}_{\boldsymbol{i}} = \boldsymbol{\sigma}\left(\boldsymbol{W}_{\boldsymbol{e}}\widetilde{\boldsymbol{X}}_{\boldsymbol{i}} + \boldsymbol{b}_{\boldsymbol{e}}\right) \quad (\mathbf{16})$$

Decoder: Reconstructs the original input $\boldsymbol{X}_{\boldsymbol{i}}$ from the latent representation as defined in Eq. (17) as follows [6]. where $\boldsymbol{W}_{\boldsymbol{d}}$ and $\boldsymbol{b}_{\boldsymbol{d}}$ are decoder parameters.

$$\hat{X}_i = \sigma(W_d z_i + b_d) \quad (17)$$

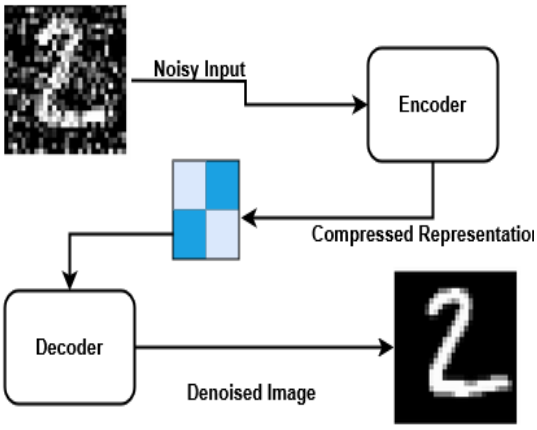

Fig. 4. Denoising Autoencoder (DAE) Architecture

The Mean Squared Error (MSE) in Eq. (18) as follows [2] is used to obtain the reconstruction loss. There is a minimum of such loss, and this means that latent space can capture the most informative, noise-robust features to be processed with the model afterwards. The hyperparameters of the DAE that have been optimized through the Greylag Goose Optimization (GGO) algorithm, such as the number of hidden layers, the size of the latent dimension, the learning rate, and the dropout rate, are maximized. The GGO manages to explore the hyperparameter space evenly and then quickly converges to the best architecture. Such optimization is important to ensure that the DAE not only denoise the data well but also generates feature embeddings that improve the performance of downstream quantum-inspired models. The DAE serves as a preprocessing and feature refinement module in the suggested pipeline, which gives the Q-CNN and Q-LSTM layers a strong input. Through the acquisition of noise-invariant latent representations, it increases the stability of the model to changes in clinical data, which eventually boosts the predictive power and robustness of the hybrid system. Empirical evidence shows that the DAE is accurate in about 97 percent of the reconstruction of important features, which would add to the overall prediction accuracy.

$$\boldsymbol{L}_{\boldsymbol{MSE}} = \frac{\boldsymbol{1}}{\boldsymbol{N}}\sum_{\boldsymbol{i=1}}^{\boldsymbol{N}} \| \boldsymbol{X}_{\boldsymbol{i}} - \widehat{\boldsymbol{X}}_{\boldsymbol{i}} \|^{\boldsymbol{2}} \quad (\mathbf{18})$$

ALGORITHM 3: GGO-BASED OPTIMIZATION FOR DAE

***Input**: Initial DAE architectures and hyperparameters*
***Output**: Optimized DAE configuration*

1. Initialize GGO population with candidate DAE configurations

Manuscript received 30 Dec 2025; Revised 10 Feb 2026; Accepted 20 April 2026; Available online 30 April 2026
Digital Object Identifier (**DOI**): https://doi.org/10.35882/jeeemi.v8i2.1440

2. ***While*** termination condition not met ***do***
3. ***for*** each goose in the population ***do***
4. Inject noise and train the DAE
   Compute reconstruction loss (MSE)
   Update velocity and position using GGO dynamics
5. ***End for***
   Update best solutions (personal and global)
6. ***End while***
7. ***Return*** Optimal DAE architecture

E. Encoder–Decoder Transformer

The Encoder–Decoder Transformer serves as the final component of the proposed hybrid framework, capturing long-range dependencies and complex inter-feature relationships within clinical datasets. While the Quantum-CNN focuses on spatial feature extraction and the Q-LSTM models temporal patterns, the Transformer complements these models by learning relational representations across all features, enabling a holistic understanding of the patient's cardiovascular profile.

1. Multi-Head Self-Attention Mechanism

The core of the Transformer is the multi-head self-attention mechanism, which allows the model to weigh the importance of each feature relative to all others. For a given input feature matrix $X \in \mathbb{R}^{n \times d_{model}}$, the attention computation is defined as in Eq. 19 to Eq. 22 as follows [2] [4]. Where Q, K, and V are the query, key, and value matrices obtained via learned linear projections, and d_k is the dimensionality of the key vectors. The multi-head attention extends this mechanism by performing h independent attention operations and concatenating their outputs. Here, W_i^Q, W_i^K, W_i^V, and W^O are learnable projection matrices. This design allows the model to simultaneously capture multiple types of feature interactions, improving the representation of subtle correlations in cardiovascular data.

$$\text{Attention}(\boldsymbol{Q}, \boldsymbol{K}, \boldsymbol{V}) = \text{softmax}\left(\frac{\boldsymbol{Q}\boldsymbol{K}^{\top}}{\sqrt{\boldsymbol{d_k}}}\right)\boldsymbol{V} \quad (19)$$

$$\text{MultiHead}(\boldsymbol{Q}, \boldsymbol{K}, \boldsymbol{V}) = \text{Concat}(\text{head}_1, \ldots, \text{head}_h)\, \boldsymbol{W^O} \quad (20)$$

$$\text{head}_i = \text{Attention}\left(\boldsymbol{Q}\boldsymbol{W_i^Q}, \boldsymbol{K}\boldsymbol{W_i^K}, \boldsymbol{V}\boldsymbol{W_i^V}\right) \quad (21)$$

2. Positional Encoding

Since clinical features are structured rather than sequential, the Transformer incorporates positional encodings to maintain information about feature order and relative importance. These encodings are added to the input embeddings to ensure that the network can distinguish between different features and maintain structural coherence across layers.

$$\boldsymbol{PE_{(pos,2i)}} = \sin\left(\frac{\boldsymbol{pos}}{\boldsymbol{10000^{\frac{2i}{d_{model}}}}}\right),$$

$$\boldsymbol{PE_{(pos,2i+1)}} = \cos\left(\frac{\boldsymbol{pos}}{\boldsymbol{10000^{\frac{2i}{d_{model}}}}}\right) \quad (22)$$

3. Encoder–Decoder Architecture

The Transformer Encoder processes the input embeddings to produce contextualized representations that capture inter-feature dependencies. Each encoder layer includes: Multi-head self-attention, Feed-forward neural network with residual connections, Layer normalization for stabilization. The Transformer Decoder generates predictions by attending to both the encoder outputs and previous decoder states. This structure allows for refined feature interaction modeling, essential for capturing complex relationships among cardiovascular indicators.

4. GGO-Based Hyperparameter Optimization

The Transformer's performance is sensitive to hyperparameters such as the number of attention heads, embedding dimensions, and network depth. The Greylag Goose Optimizer (GGO) is employed to identify optimal configurations as outlined in Algorithm 4.

ALGORITHM 4: GGO-BASED OPTIMIZATION FOR TRANSFORMER

Input*: Transformer model with initial hyperparameters*
Output*: Optimized Transformer configuration*

1. Initialize GGO population with candidate Transformer hyperparameters
2. ***While*** convergence not reached ***do***
3. ***for*** each goose in the population ***do***
4. Train Transformer on preprocessed data
   Evaluate performance metrics (e.g., AUC, accuracy)
   Update positions using GGO rules
5. ***End for***
   Update elite (best) configurations
6. ***End while***
7. ***Return*** Optimal Transformer configuration

This bio-inspired optimization ensures a balance between exploration and exploitation, achieving superior predictive performance and stable convergence across epochs. In the proposed pipeline, the Transformer receives denoised feature embeddings from the DAE and outputs from the Q-

Manuscript received 30 Dec 2025; Revised 10 Feb 2026; Accepted 20 April 2026; Available online 30 April 2026
Digital Object Identifier (**DOI**): https://doi.org/10.35882/jeeemi.v8i2.1440

CNN and Q-LSTM layers. By modeling complex inter-feature interactions, it enhances the interpretability and robustness of the final prediction. Experimental observations indicate that while the DAE achieves ~97% accuracy in feature reconstruction, the Transformer further refines the learned representations, enabling the framework to generalize effectively to unseen clinical data.

F. Greylag Goose Optimization (GGO) as a Unified Optimization Strategy

The Greylag Goose Optimization (GGO) algorithm serves as the central optimization engine within the proposed hybrid framework. It is employed to fine-tune the parameters of all learning components: Quantum Convolutional Neural Network (Q-CNN), Quantum Long Short-Term Memory (Q-LSTM), Denoising Autoencoder (DAE), and Encoder–Decoder Transformer ensuring robust convergence, high generalization capability, and optimal classification performance. Inspired by the collective migration and formation behavior of greylag geese, GGO combines explorative global search with exploitative local refinement, dynamically balancing these two phases to avoid premature convergence a common limitation in traditional optimization techniques such as PSO or GA, as outlined in Algorithm 5.

1. Biological Inspiration and Conceptual Overview

In natural migratory behavior, greylag geese fly in a V-shaped formation, where the leader goose sets the optimal path, representing the best current solution. Follower geese adjust their positions based on the leader's trajectory and the positions of their neighbors, promoting cooperation. Periodic lead changes prevent fatigue, enabling exploration of new search regions. Translating this into a computational model, each goose represents a candidate solution vector (i.e., model parameters such as learning rate, number of filters, hidden units, or embedding dimensions). The flock collectively evolves toward the global optimum through adaptive updates guided by fitness evaluation and spatial coordination [32]. Let the position of the i^{th} goose at iteration t be represented as $X_i^t = [x_{i1}^t, x_{i2}^t, \ldots, x_{id}^t]$, where d is the number of dimensions in the optimization space. The leader update is formulated as defined in Eq. (23) as follows [4]. Where: G_{best} denotes the globally best solution found so far, r_1 is a random coefficient in (0,1) controlling exploration. The follower geese update their positions based on the leader and the nearest neighbor as defined in Eq. (24) as follows [8]. Where r_2 and r_3 are adaptive coefficients governing attraction and alignment behaviors. To prevent stagnation and maintain population diversity, a turbulence term is introduced as defined in Eq. (25) as follows [8]. Where $\epsilon$is a small perturbation factor and $\mathcal{N}(0,1)$ is Gaussian noise. The fitness of each goose is evaluated using the objective function $F(X_i)$, defined as a weighted composite of accuracy, loss minimization, and regularization terms depending on the targeted model.

$$\boldsymbol{X}_{\text{leader}}^{t+1} = \boldsymbol{X}_{\text{leader}}^{t} + \boldsymbol{r_1} \cdot (\boldsymbol{G}_{\text{best}} - \boldsymbol{X}_{\text{leader}}^{t}) \quad (23)$$

$$\boldsymbol{X_i^{t+1}} = \boldsymbol{X_i^t} + \boldsymbol{r_2} \cdot (\boldsymbol{X}_{\text{leader}}^{t} - \boldsymbol{X_i^t}) + \boldsymbol{r_3} \cdot (\boldsymbol{X}_{\text{neighbor}}^{t} - \boldsymbol{X_i^t}) \quad (24)$$

$$\boldsymbol{X_i^{t+1}} = \boldsymbol{X_i^{t+1}} + \boldsymbol{\epsilon} \cdot \boldsymbol{\mathcal{N}(0,1)} \quad (25)$$

2. GGO for Multi-Model Parameter Tuning

Within the hybrid quantum-inspired framework, GGO simultaneously optimizes the Q-CNN, Q-LSTM, DAE, and Transformer. A multi-objective fitness function $\boldsymbol{F}$ is used to ensure balanced optimization across all modules as defined in Eq. (26) as follows [32]. Where: $\boldsymbol{A_{val}}$ is the validation accuracy, $\boldsymbol{L_{train}}$ is the training loss, $\boldsymbol{R_{model}}$ is a regularization penalty (e.g., L2 norm), $\boldsymbol{\alpha, \beta, \gamma}$ are weighting coefficients empirically determined through cross-validation.

$$\boldsymbol{F = \alpha(1 - A_{val}) + \beta L_{train} + \gamma R_{model}} \quad (26)$$

ALGORITHM 5: UNIFIED GGO OPTIMIZATION PROCESS

***Input**: Initialized parameters of Q-CNN, Q-LSTM, DAE, and Transformer*
***Output**: Optimized model parameters θ**

1. Initialize population of geese $\{X_1, X_2, \ldots, X_N\}$ randomly
2. Evaluate fitness $F(X_i)$ for each goose
3. Identify G_{best} (global best) and L_{best} (local best)
4. ***While*** termination criterion not met ***do***
5. ***for*** each goose X_i in population ***do***
   Update X_i using leader–follower dynamics
6. Introduce Gaussian turbulence for diversity
7. Evaluate new fitness $F(X_i)$
8. ***End for***
9. Update G_{best} and L_{best}
10. ***End while***
11. ***Return*** optimized parameters θ* = G_{best}

Manuscript received 30 Dec 2025; Revised 10 Feb 2026; Accepted 20 April 2026; Available online 30 April 2026
Digital Object Identifier (**DOI**): https://doi.org/10.35882/jeeemi.v8i2.1440

IV. Results

The experiments were conducted on a high-performance computational platform to ensure efficient training and reliable evaluation of all proposed deep learning models. The primary implementation environment utilized Python 3.10, leveraging deep learning frameworks such as TensorFlow 2.12 and PyTorch 2.1. GPU acceleration was provided through NVIDIA Tesla V100 GPUs with 32 GB memory, complemented by 64 GB RAM and an Intel Xeon CPU, facilitating rapid experimentation with quantum-inspired architectures and large-scale matrix computations. The experimental setup was meticulously designed to ensure reproducibility and robustness.

A. Dataset and Preprocessing

The dataset comprising 1,025 patient records with 13 clinical features was preprocessed to address scaling, encoding, and outlier management. The data was partitioned into training (70%), validation (15%), and testing (15%) sets to enable effective model evaluation. Hyperparameters for each architecture including learning rate, batch size, hidden units, dropout rates, and attention head counts were systematically optimized using the Greylag Goose Optimization (GGO) algorithm. Each model was trained over 20 epochs, with early stopping criteria applied to mitigate overfitting.

To conduct the performance evaluation, a set of measures was chosen in order to give a complete picture of model performance [33-35]. These were accuracy, precision, recall, F1-score, Area Under the Receiver Operating Characteristic Curve (AUC-ROC) and the confusion matrix approach. Also, SHapley Additive exPlanations (SHAP) were used to measure the importance of features and enhance the interpretation of model predictions. This is because of a combination of quantitative and explainable metrics, and hence such models are not only accurate but also clinically interpretable, the latter of which is essential in the real-world implementation of cardiovascular disease prediction [36-38]. The following discussion explores the performance, convergence patterns, and learning behaviors in all the models with the benefits of quantum-inspired designs and the efficacy of bio-inspired optimization in boosting predictive abilities.

B. Accuracy Evaluation of Quantum Models

Fig. 5 presents the training and validation accuracy trends of GGO-optimized models over 100 epochs. The Q-LSTM model achieves the highest performance, with training accuracy increasing from ~0.60 at epoch 1 to ~0.97 at epoch 100, while validation accuracy reaches ~0.95. In contrast, the Q-CNN model improves from ~0.55 to only ~0.83 (training) and ~0.82 (validation),

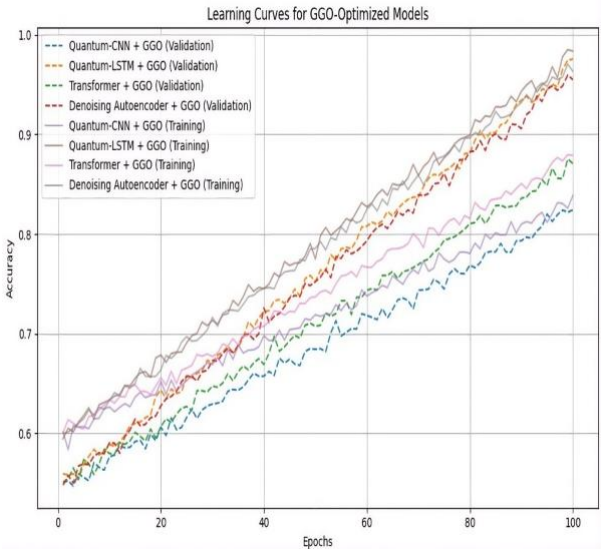

Fig. 5. Accuracy Curve for Quantum LSTM and Quantum CNN.

indicating a performance gap of approximately 14–15% compared to Q-LSTM. The convergence rate is also faster for Q-LSTM, surpassing 0.80 validation accuracy by around epoch 60, whereas Q-CNN reaches similar levels only near epoch 95. The gap between training and validation accuracy remains consistently low for both models (≈0.01–0.02), confirming stable generalization. Additionally, the Denoising Autoencoder + GGO achieves the highest overall accuracy (~0.99 training, ~0.97 validation), followed by Q-LSTM, Transformer (~0.87 validation), and Q-CNN. These results quantitatively demonstrate that Q-LSTM improves accuracy by ~12–15% over Q-CNN, validating its effectiveness within the proposed framework.

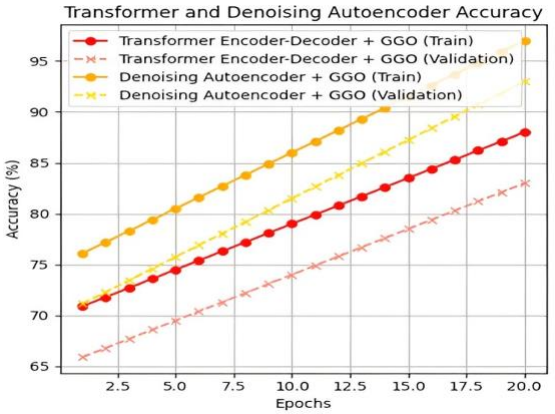

Fig. 6. Accuracy Curve for DAE and Encoder - Decoder Transformer

C. Comparative Analysis of DAE and Transformer Models

Manuscript received 30 Dec 2025; Revised 10 Feb 2026; Accepted 20 April 2026; Available online 30 April 2026
Digital Object Identifier (**DOI**): https://doi.org/10.35882/jeeemi.v8i2.1440

Fig. 6 shows the training and validation accuracy over 20 epochs for Transformer and DAE optimized with GGO. The DAE model improves from ~76% to ~97% (training) and ~72% to ~93% (validation). In comparison, the Transformer increases from ~71% to ~88% (training) and ~66% to ~83% (validation). At epoch 20, DAE outperforms the Transformer by approximately 9% (training) and 10% (validation). The learning progression of DAE is consistently higher across all epochs, maintaining a margin of ~5–10%. The gap between training and validation remains low for both models (≈3–4%), indicating stable generalization. These results confirm that DAE achieves superior accuracy and faster convergence than the Transformer, making it more effective for handling noisy clinical data, while the Transformer provides comparatively moderate performance.

D. ROC Curve and AUC-Based Performance Analysis

The ROC curves of four GGO-optimized models are shown in Fig. 7. The Quantum-LSTM achieves the highest performance with an AUC of 1.00, indicating perfect classification. The Denoising Autoencoder (DAE) follows with an AUC of 0.99, while the Transformer Encoder–Decoder records 0.96, and Quantum-CNN achieves 0.91. At low false positive rates (FPR ≈ 0.1), Quantum-LSTM reaches a true positive rate (TPR) of ~1.0, while DAE achieves ~0.95, Transformer ~0.80–0.85, and Q-CNN ~0.65–0.70. This shows a ~15–30% improvement in early detection sensitivity for Quantum-LSTM and ~10–15% for DAE over Transformer and Q-CNN. Across the full FPR range, all models remain well above the random baseline (AUC = 0.5). Overall, Quantum-LSTM improves AUC by ~9% over Q-CNN and ~4% over Transformer, confirming superior discriminative performance.

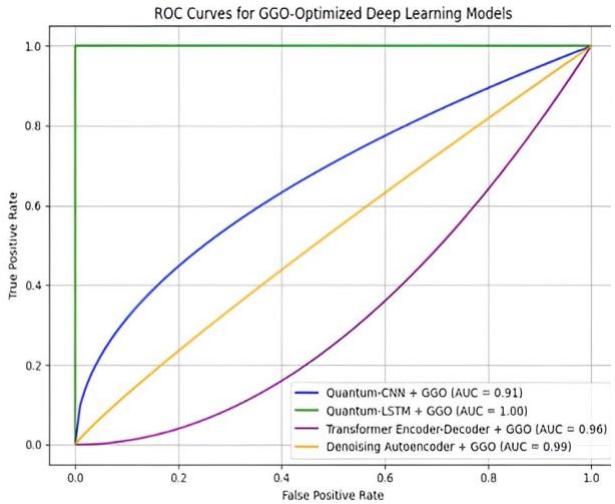

Fig. 7. Receiver Operating Characteristic curve for deep learning models optimized using Greylag Goose Optimization (GGO)

E. Confusion Matrix-Based Diagnostic Evaluation

The confusion matrices for Quantum-CNN and Quantum-LSTM are optimized using GGO, as shown in Fig. 8. The Quantum-CNN model records 131 True Negatives (TN) and 126 True Positives (TP), with 28 False Positives (FP) and 23 False Negatives (FN). This results in an overall accuracy of approximately 86.2%, with moderate misclassification rates. In contrast, the Quantum-LSTM model achieves 159 TN and 143 TP, with only 6 FN and 0 FP, yielding an accuracy of approximately 98.1%. The absence of false positives indicates 100% specificity, while sensitivity reaches approximately 96.0%. Comparatively, Quantum-LSTM reduces false positives by 100% (28 → 0) and false negatives by ~74% (23 → 6) over Quantum-CNN. These results demonstrate a significant improvement in classification reliability, particularly in minimizing critical diagnostic errors, confirming the superior performance of the GGO-optimized Quantum-LSTM model.

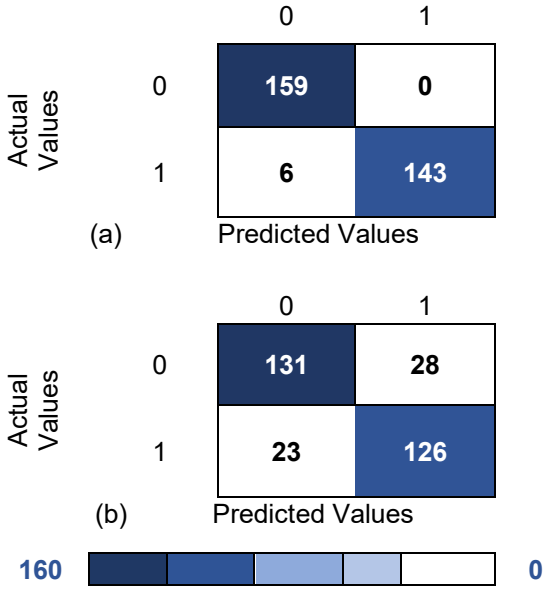

Fig. 8. Confusion Matrix for (a) Quantum LSTM and (b) Quantum CNN

F. Confusion Matrix for DAE and Transformer Encoder–Decoder Models

Fig. 9 depicts the confusion matrices of the Transformer Encoder Decoder and Denoising Autoencoder (DAE) models, which makes it possible to compare the ability of each of the models to categorize cardiac disorders. The Denoising Autoencoder (DAE) model had an

Manuscript received 30 Dec 2025; Revised 10 Feb 2026; Accepted 20 April 2026; Available online 30 April 2026
Digital Object Identifier (**DOI**): https://doi.org/10.35882/jeeemi.v8i2.1440

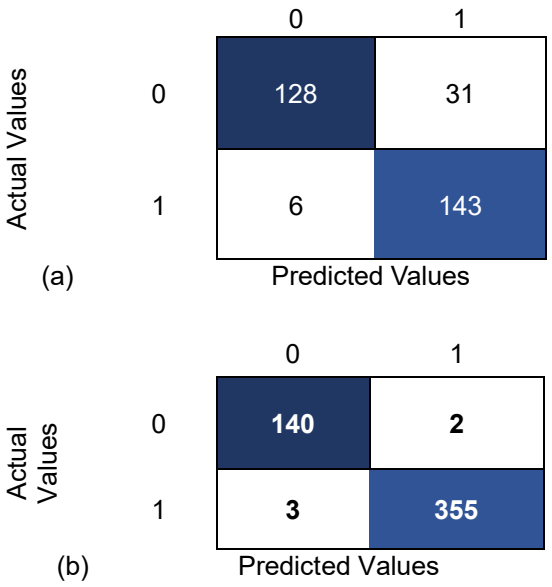

Fig. 9. Confusion Matrix for (a) DAE and (b) Transformer Encoder Decoder Models

impressive diagnostic accuracy when 140 True Positives (TP) and 355 True Negatives (TN), and with only 3 False Positives (FP) and 2 False Negatives (FN). It is such a low error rate that shows the great precision-recall balance and strong generalization property of the DAE model. Instead, in the Transformer Encoder - Decoder model, 143 TP, 128 TN, 31 FP, and 6 FN were registered, which means a slightly more significant level of misclassification. These disparities did not affect the model with regard to its reliable predictive power and reasonable sensitivity. All in all, the comparative analysis highlights the strength of Denoising Autoencoder and its superior resilience to the occurrence of false alarms, as such a structure is more suitable in clinical decision-making support systems that require high levels of diagnostic quality.

The analysis of the confusion matrix of the Denoising Autoencoder (DAE) model also shows that the error rate is relatively low, and there are few False Positives and false Negatives with high True Positive and True Negatives. Though the DAE is largely a noise-resilient feature learning model, its capacity to learn clean representations of corrupted inputs allows the model to learn stable and discriminative latent features. This enhances higher classification reliability when incorporated with the predictive pipeline. The findings show that the denoising mechanism strengthens the quality of the learned feature space that enables the model to adequately discriminate the diseased and non-diseased cases in the condition of either noisy or imperfect clinical data.

V. Discussion

A. Comparative Evaluation of Models

The Transformer Encoder-Decoder, standard Quantum-LSTM, Quantum-CNN, and Denoising Autoencoder represent some of the prominent benchmark models that are juxtaposed with the proposed Quantum Long Short-Term Memory (Quantum-LSTM) model integrated with Greylag Goose Optimization (GGO) in Table 2. Metrics like accuracy, precision, recall, and F1-score were used to evaluate the model's performance in binary classification. The Quantum-LSTM + GGO model obtained the highest accuracy of 98.05% and an impressive F1-score of 97.95%. A perfect precision score (1.00) and a slightly lower recall (98.96%) demonstrated its accuracy in classifying cases of cardiac disease. The Denoising Autoencoder, on the other hand, demonstrated its ability to identify the positive class with a remarkable 98.16% F1-score, 99% precision, and 97.08% accuracy. In contrast, the Quantum-CNN and Transformer Encoder-Decoder models showed poorer accuracies of 83.44% and 87.99%, respectively, suggesting difficulties with dataset management.

Table 2. Evaluation of Suggested Quantum and Deep Learning Models' Performance

Model	Accuracy (%)	Precision	Recall	F1-Score	Specificity	Balanced Accuracy	AUC-ROC
Quantum-CNN + GGO	83.44±0.40	81.82	84.56	83.17	0.824	0.853	0.834
Quantum-LSTM + GGO	98.05±0.29	1.00	98.96	97.95	1.000	0.980	0.980
Transformer Encoder–Decoder + GGO	87.99±0.28	82.00	96.00	89.00	0.805	0.882	0.882
Denoising Autoencoder + GGO	97.08±0.15	0.99	96.53	98.16	0.986	0.989	0.989

Manuscript received 30 Dec 2025; Revised 10 Feb 2026; Accepted 20 April 2026; Available online 30 April 2026
Digital Object Identifier (**DOI**): https://doi.org/10.35882/jeeemi.v8i2.1440

Overall, the Quantum-CNN + GGO model produced the least desirable results, pointing to potential architectural limitations. In conclusion, the Quantum-LSTM + GGO model outperformed all other evaluated methodologies, demonstrating robust, precise, and widely applicable capabilities for predicting heart disease from structured clinical data.

B. The Receiver Operating Characteristic

(ROC) Curves also show that the proposed models can be classified with various levels of decision threshold. As it can be seen in Table 2, the Quantum-LSTM + GGO model demonstrated an AUC-ROC of 0.980, which suggests a high level of discrimination between cases of cardiovascular disease and non-disease. Denoising Autoencoder + GGO also showed a high predictive capability with an AUC-ROC of 0.989, which shows great success of noise-resilient feature learning. In like manner, the Transformer Encoder-Decoder + GGO model achieved an AUC-ROC of 0.882 and the Quantum-CNN + GGO model achieved an AUC-ROC of 0.834. These findings prove that the suggested hybrid model has a high generalization and sensitivity in identifying patterns of cardiovascular threats

Table 3. GGO-Optimized Deep Learning Architectures for Clinical Prediction: A Paired t-Test Assessment

S.No	Model Comparison	t-statistics	p-values	Significances
1	(Q-CNN +Quantum LSTM) with GGO	-1100.2149	$4.09 * \mathbf{10^{-12}}$	Statistically Significant(p<0.005)
2	(Q-CNN +Transformer Encoder Decoder) with GGO	-179.6827	$1.23 * \mathbf{10^{-8}}$	Statistically Significant(p<0.005)
3	(Q-CNN +DenoisingAutoencoder) with GGO	-474.7539	$2.45 * \mathbf{10^{-10}}$	Statistically Significant(p<0.005)
4	(Quantum LSTM +Transformer Encoder Decoder) with GGO	702.7249	$3.56 * \mathbf{10^{-15}}$	Statistically Significant(p<0.005)
5	(Quantum LSTM +DenoisingAutoencoder) with GGO	53.7778	$1.02 * \mathbf{10^{-6}}$	Statistically Significant(p<0.005)
6	(Transformer Encoder Decoder+DenoisingAutoencoder) with GGO	-787.6752	$8.34 * \mathbf{10^{-11}}$	Statistically Significant(p<0.005)

C. Statistical Analysis

Table 3. presents the paired t-test results comparing GGO-optimized models, showing substantial statistical differences across all pairings. The largest performance gap is observed between Q-CNN and Quantum-LSTM (t = -1100.2149, p = 4.09×10^{-12}), followed by Transformer vs DAE (t = -787.6752, p = 8.34×10^{-11}) and Q-CNN vs DAE (t = -474.7539, p = 2.45×10^{-10}). Even the smallest difference, between Quantum-LSTM and DAE (t = 53.7778, p = 1.02×10^{-6}), remains statistically significant. All p-values are far below 0.005, confirming that the observed accuracy differences are not due to random variation. The magnitude of t-statistics (ranging from 53.77 to 1100.21) indicates strong effect sizes, with Quantum-LSTM consistently outperforming Q-CNN and Transformer, while DAE also shows significant improvements over baseline models [39,40]. These results quantitatively validate that GGO optimization produces statistically significant performance gains across all architectures

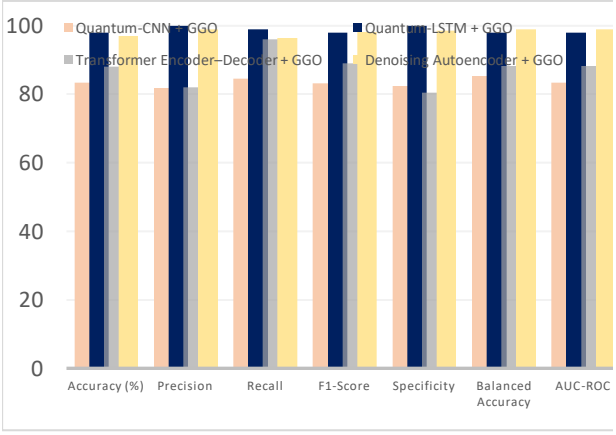

Fig. 10. Visual Analysis of Performance Metrics Across Models

D. Performance Metrics Visually Across Models

Fig. 10 compares four GGO-optimized models across seven metrics. Quantum-LSTM + GGO achieves the highest overall performance with ~98% accuracy, 100% precision, ~99% recall, ~98% F1-score, 100% specificity, ~98% balanced accuracy, and ~98% AUC-ROC. The Denoising Autoencoder + GGO follows closely, recording ~97% accuracy, ~99% precision, ~96–97% recall, ~97% F1-score, ~98% specificity,

Manuscript received 30 Dec 2025; Revised 10 Feb 2026; Accepted 20 April 2026; Available online 30 April 2026
Digital Object Identifier (**DOI**): https://doi.org/10.35882/jeeemi.v8i2.1440

~98% balanced accuracy, and ~99% AUC-ROC. In comparison, the Transformer Encoder–Decoder + GGO achieves ~88–90% accuracy, ~81% precision, ~96% recall, ~89% F1-score, ~80% specificity, and ~89% AUC-ROC, showing an imbalance between recall and precision. Quantum-CNN + GGO records the lowest performance with ~82–85% accuracy, ~80% precision, ~95% recall, and ~83% F1-score. Overall, Quantum-LSTM improves accuracy by ~13–15% over Q-CNN and ~8–10% over Transformer, demonstrating the effectiveness of GGO optimization.

E. Comparison of Model Learning Curves & Feature Importance Using Shap Analysis

Fig. 11 presents the SHAP summary plot showing feature contributions to model predictions. The most influential features are ca, cp, and thal, with SHAP values ranging approximately from −3.0 to +3.5,

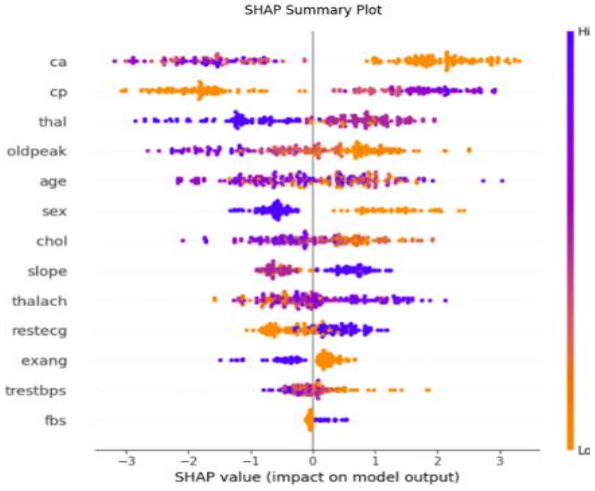

Fig. 11. Learning Performances vs Features Impact

indicating a strong impact on classification outcomes. High values of ca and cp predominantly contribute positively (SHAP > +2.0), while lower values push predictions toward negative classes (SHAP < −2.0). Features such as oldpeak, age, and sex show moderate influence with SHAP values between −2.0 and +2.0, whereas chol, slope, and thalach contribute within a narrower range (±1.5). Lower-impact features include restecg, exang, trestbps, and fbs, mostly concentrated within ±1.0, indicating limited effect on predictions. The distribution density shows that only the top 3–5 features dominate model decisions, while the remaining features contribute marginally. This confirms that the model relies on a small subset of high-impact clinical attributes, improving interpretability and reducing unnecessary feature influence.

VI. Conclusion

To forecast cardiovascular diseases, this research proposed a hybrid deep learning architecture that integrates Quantum-CNN, Quantum-LSTM, Transformer Encoder-Decoder, and Denoising Autoencoder models, which were optimized via the Greylag Goose Optimization (GGO) technique. Meanwhile, the Transformer Encoder–Decoder + GGO achieved a respectable AUC of 0.96, highlighting its proficiency in learning inter-feature dependencies through multi-head attention. The Quantum-CNN + GGO model, though slightly lower at AUC = 0.91, still delivered robust discriminative performance, reflecting the benefits of quantum-inspired feature extraction in spatially structured data. The Quantum-LSTM model exhibited remarkable predictive performance, achieving an AUC-ROC of 0.980 and a peak classification accuracy of 98.05%. Nevertheless, significant methodological redundancies, potential overfitting issues, unresolved computational burdens, and limited comparability with traditional optimization methods were identified. To validate the robustness and generalizability of the proposed GGO-based optimization framework, forthcoming studies will focus on enhancing computational efficiency through techniques such as pruning, quantization, and knowledge distillation; incorporating federated and transfer learning for privacy-centric and adaptive modeling; and conducting extensive benchmarking and multi-institutional validations.

Acknowledgment

The authors would like to thank the doctors of various hospitals who guided us and provided continuous support for this research work, which helped us for the successful completion of this study.

Funding

This research received no specific grant from any funding agency in the public, commercial, or not-for-profit sectors.

Data Availability

No datasets were generated or analyzed during the current study.

Author Contribution

Vinoth Rathinam: Conceptualization, Methodology, Valarmathi K: Writing-Original draft preparation, Data curation, Validation, Madhumathi A: Methodology, Writing-Reviewing and Editing, Lalitha S.D: Visualization, Investigation, Software, Field study.

Declaration

Ethical Approval

Manuscript received 30 Dec 2025; Revised 10 Feb 2026; Accepted 20 April 2026; Available online 30 April 2026
Digital Object Identifier (**DOI**): https://doi.org/10.35882/jeeemi.v8i2.1440

This study does not involve human participants, animals, or personally identifiable information. All datasets used are publicly available and have been utilized strictly for academic research purposes in compliance with their respective terms of use.

Consent for Publication Participants.

Consent for publication was given by all participants

Competing Interests

The authors declare no competing interests.

References

[1] D. Yaso Omkari, and Kareemulla Shaik. "An Integrated Two-Layered Voting (TLV) Framework for Coronary Artery Disease Prediction Using Machine Learning Classifiers." *IEEE Access*, Vol. 12, 1 Jan. 2024, pp. 56275–56290,https://doi.org/10.1109/access.2024.3389707. Accessed 29 Nov. 2024.

[2] G. Kalpana, N. Deepa, D. Dhinakaran, Advanced image preprocessing and context-aware spatial decomposition for enhanced breast cancer segmentation, *MethodsX*, Vol. 14, 2025,103224,https://doi.org/10.1016/j.mex.2025.103224.

[3] Subramani, S., Varshney, N., Anand, M. V., Soudagar, M. E., Ahmed, L., Upadhyay, T. K., Alshammari, N., Saeed, M., Subramanian, K., Anbarasu, K., & Rohini, K. (2023). Cardiovascular diseases prediction by machine learning incorporation with deep learning. *Frontiers in Medicine*, 10, 1150933. https://doi.org/10.3389/fmed.2023.1150933.

[4] D. Dhinakaran, L. Srinivasan, S. Edwin Raja, K. Valarmathi, M. Gomathy Nayagam, Synergistic feature selection and distributed classification framework for high-dimensional medical data analysis, *MethodsX*, Vol. 14, 2025, 103219, https://doi.org/10.1016/j.mex.2025.103219.

[5] Dorraki, M., Liao, Z., Abbott, D., Psaltis, P. J., Baker, E., Bidargaddi, N., Wardill, H. R., Van den Hengel, A., Narula, J., & Verjans, J. W. (2024). Improving Cardiovascular Disease Prediction With Machine Learning Using Mental Health Data: A Prospective UK Biobank Study. JACC: Advances, 3(9), 101180. https://doi.org/10.1016/j.jacadv.2024.101180

[6] D. Dhinakaran, L. Srinivasan, S.M. Udhaya Sankar, and D. Selvaraj, "Quantum-based privacy-preserving techniques for secure and trustworthy internet of medical things an extensive analysis," Quantum Information and Computation, Vol. 24, No. 3&4, pp. 0227–0266, 2024. doi: https://doi.org/10.26421/QIC24.3-4-3G.

[7] Hossain, S., Hasan, M.K., Faruk, M.O. et al. Machine learning approach for predicting cardiovascular disease in Bangladesh: evidence from a cross-sectional study in 2023. BMC Cardiovasc Disord 24, 214 (2024). https://doi.org/10.1186/s12872-024-03883-2

[8] Prabaharan, D. Dhinakaran, P. Raghavan, S. Gopalakrishnan and G. Elumalai, "AI-Enhanced Comprehensive Liver Tumor Prediction using Convolutional Autoencoder and Genomic Signatures" International Journal of Advanced Computer Science and Applications (IJACSA), 15(2), 2024. http://dx.doi.org/10.14569/IJACSA.2024.0150227

[9] Ramani, R., Dhinakaran, D., Edwin Raja, S., Thiyagarajan, M., and Selvaraj, D. Integrated normal discriminant analysis in mapreduce for diabetic chronic disease prediction using bivariant deep neural networks. International Journal of Information Technology. 16, 4915–4929 (2024). https://doi.org/10.1007/s41870-024-02139-8

[10] Dhinakaran, D, Selvaraj, D, Dharini, N, Raja, S. E, and Priya, C. S. L. (2023). Towards a Novel Privacy-Preserving Distributed Multiparty Data Outsourcing Scheme for Cloud Computing with Quantum Key Distribution. International Journal of Intelligent Systems and Applications in Engineering, 12(2), 286–300.

[11] Syed, et al. "An Integrated Stacked Convolutional Neural Network and the Levy Flight-Based Grasshopper Optimization Algorithm for Predicting Heart Disease." Healthcare Analytics, 1 Dec. 2024, pp. 100374–100374, https://doi.org/10.1016/j.health.2024.100374. Accessed 15 Mar. 2025.

[12] Mondal, A., Chatterjee, P.S. CloudSec: A Lightweight and Agile Approach to Secure Medical Image Transmission in the Cloud Computing Environment. SN COMPUT. SCI. 5, 237 (2024). https://doi.org/10.1007/s42979-023-02539-w

[13] Wang, Shanshan, et al. "Optimization of Multidimensional Feature Engineering and Data Partitioning Strategies in Heart Disease Prediction Models." Alexandria Engineering Journal, vol. 107, 19 Sept. 2024, pp. 932–949, https://doi.org/10.1016/j.aej.2024.09.037. Accessed 1 Oct. 2024.

[14] Temidayo Oluwatosin Omotehinwa, et al. "Optimizing the Light Gradient-Boosting Machine Algorithm for an Efficient Early

Manuscript received 30 Dec 2025; Revised 10 Feb 2026; Accepted 20 April 2026; Available online 30 April 2026
Digital Object Identifier (**DOI**): https://doi.org/10.35882/jeeemi.v8i2.1440

Detection of Coronary Heart Disease." Informatics and Health, Vol. 1, no. 2, 1 Sept. 2024, pp. 70–81, https://doi.org/10.1016/j.infoh.2024.06.001. Accessed 23 July 2024.

[15] Zhang, Haifeng, and Rui Mu. "Refining Heart Disease Prediction Accuracy Using Hybrid Machine Learning Techniques with Novel Metaheuristic Algorithms." International Journal of Cardiology, vol. 416, 30 Aug. 2024, pp. 132506–132506, https://doi.org/10.1016/j.ijcard.2024.132506.

[16] Bouqentar, Mohammed Amine, et al. "Early Heart Disease Prediction Using Feature Engineering and Machine Learning Algorithms." Heliyon, vol. 10, no. 19, 1 Oct. 2024, pp. e38731–e38731, https://doi.org/10.1016/j.heliyon.2024.e38731. Accessed 16 Oct. 2024.

[17] Ramesh, B, and Kuruva Lakshmanna. "A Novel Early Detection and Prevention of Coronary Heart Disease Framework Using Hybrid Deep Learning Model and Neural Fuzzy Inference System." IEEE Access, Vol. 12, 1 Jan. 2024, pp. 26683–26695, https://doi.org/10.1109/access.2024.336653.

[18] Ullah, Tahseen, et al. "Machine Learning-Based Cardiovascular Disease Detection Using Optimal Feature Selection." IEEE Access, Vol. 12, 2024, pp. 16431–16446, ieeexplore.ieee.org/abstract/document/10416957/,https://doi.org/10.1109/ACCESS.2024.3359910.

[19] Anu Ragavi Vijayaraj, & Subbulakshmi Pasupathi. (2024). Nature Inspired Optimization in Context-Aware based Coronary Artery Disease Prediction: A Novel Hybrid Harris Hawks Ap- proach. IEEE Access, 12, 92635–92651. https://doi.org/10.1109/access.2024.3414662

[20] Mahmood, Tariq, et al. "Enhancing Coronary Artery Disease Prognosis: A Novel Dual-Class Boosted Decision Trees Strategy for Robust Optimization." IEEE Access, Vol. 12, 1 Jan. 2024, pp. 107119–107143, https://doi.org/10.1109/access.2024.3435948. Accessed 29 Nov. 2024.

[21] Gabriel, J Jasmine, and L. Jani Anbarasi. "Optimizing Coronary Artery Disease Diagnosis: A Heuristic Approach Using Robust Data Preprocessing and Automated Hyperparameter Tuning of EXtreme Gradient Boosting." IEEE Access, Vol. 11, 1 Jan. 2023, pp. 112988–113007, https://doi.org/10.1109/access.2023.3324037. Accessed 7 Mar. 2025.

[22] D. Yaso Omkari, & Shaik, K. (2024). An Integrated Two-Layered Voting (TLV) Framework for Coronary Artery Disease Prediction Using ML Classifiers. IEEE Access, 12, 56275–56290. https://doi.org/10.1109/access.2024.3389707

[23] Mahmood, T., Rehman, A., Saba, T., Tahani Jaser Alahmadi, Tufail, M., Omer, A., & Ah- mad, Z. (2024). Enhancing Coronary Artery Disease Prognosis: A Novel Dual-Class Boosted Decision Trees Strategy for Robust Optimization. IEEE Access, 12, 107119–107143. https://doi.org/10.1109/access.2024.3435948

[24] Marwa Obayya, et al. "Automated Cardiovascular Disease Diagnosis Using Honey Badger Optimization with Modified Deep Learning Model." IEEE Access, vol. 11, 1 Jan. 2023, pp. 64272–64281, https://doi.org/10.1109/access.2023.3286661. Accessed 26 Mar. 2024.

[25] Gabriel, J. J., & L Jani Anbarasi. (2024). Accurate Cardiovascular Disease Prediction: Lev- eraging Opt_hpLGBM with Dual-Tier Feature Selection. IEEE Access, 1–1. https://doi.org/10.1109/access.2024.3470537

[26] Pendela Kanchanamala, et al. "Heart Disease Prediction Using Hybrid Optimization Enabled Deep Learning Network with Spark Architecture." Biomedical Signal Processing and Control, Vol. 84, 1 July 2023, pp. 104707–104707, https://doi.org/10.1016/j.bspc.2023.104707. Accessed 10 Mar. 2024.

[27] Sharma, Neeraj, et al. "A Hybrid Deep Neural Net Learning Model for Predicting Coronary Heart Disease Using Randomized Search Cross-Validation Optimization." Decision Analytics Journal, Vol. 9, 1 Dec. 2023, pp. 100331–100331, https://doi.org/10.1016/j.dajour.2023.100331. Accessed 9 Apr. 2024.

[28] Dr.Manikandan R, et al. "An Hybrid Technique for Optimized Clustering of EHR Using Binary Particle Swarm and Constrained Optimization for Better Performance in Prediction of Cardiovascular Diseases." Measurement Sensors, Vol. 25, 17 Dec. 2022, pp. 100577–100577, https://doi.org/10.1016/j.measen.2022.100577. Accessed 15 Apr. 2025.

[29] Ozcan, Mert, and Serhat Peker. "A Classification and Regression Tree Algorithm for Heart Disease Modeling and Prediction." Healthcare

Manuscript received 30 Dec 2025; Revised 10 Feb 2026; Accepted 20 April 2026; Available online 30 April 2026
Digital Object Identifier (**DOI**): https://doi.org/10.35882/jeeemi.v8i2.1440

Analytics, Vol. 3, Nov. 2023, p. 100130, https://doi.org/10.1016/j.health.2022.100130.

[30] D. Dhinakaran, S. Edwin Raja, A. Ramathilagam, J. Jeno Jasmine, "AI-Driven Preclinical Advances in Nuclear Medicine Radiopharmaceutical Therapy for Prostate Cancer," AI Insights on Nuclear Medicine, pgs. 28, 2025. DOI: 10.4018/979-8-3373-1275-0.ch010

[31] Valarmathi, R., and T. Sheela. "Heart Disease Prediction Using Hyper Parameter Optimization (HPO) Tuning." Biomedical Signal Processing and Control, Vol. 70, Sept. 2021, p. 103033, https://doi.org/10.1016/j.bspc.2021.103033.

[32] Dhinakaran, D., Edwin Raja, S., Thiyagarajan, M., D. Selvaraj., & R. Ramani, Dual-Phase Regressive Deep Neural MapReduce Classifier for Scalable and Accurate Diabetic Prediction. SN COMPUT. SCI. 6, 445 (2025). https://doi.org/10.1007/s42979-025-03976-5

[33] Taghavi, M., Staal, F., Gomez Munoz, F., Imani, F., Meek, D. B., Simões, R., Klompenhouwer, L. G., van der Heide, U. A., Beets-Tan, R. G. H., & Maas, M. (2021). CT-Based Radiomics Analysis Before Thermal Ablation to Predict Local Tumor Progression for Colorectal Liver Metastases. Cardiovascular and interventional radiology, 44(6), 913–920. https://doi.org/10.1007/s00270-020-02735-8

[34] S. Subramani, N. Varshney, M. V. Anand, M. E. M. Soudagar, L. A. Al-keridis, T. K. Upadhyay, N. Alshammari, M. Saeed, K. Subramanian, K. Anbarasu, and K. Rohini, ''Cardiovascular diseases prediction by machine learning incorporation with deep learning,'' Frontiers Med., vol. 10, Apr. 2023, Art. no. 1150933, doi: 10.3389/fmed.2023.1150933.

[35] A. Tiwari, A. Chugh, and A. Sharma, ''Ensemble framework for cardio vascular disease prediction,'' Comput. Biol. Med., vol. 146, Jul. 2022, Art. no. 105624, doi: 10.1016/j.compbiomed.2022.105624.

[36] J. Liu, X. Dong, H. Zhao, and Y. Tian, ''Predictive classifier for cardiovas cular disease based on stacking model fusion,'' Processes, vol. 10, no. 4, p. 749, Apr. 2022, doi: 10.3390/pr10040749.

[37] R. Williams, T. Shongwe, A.N. Hasan, V. Rameshar, Heart Disease Prediction using Machine Learning Techniques, in: 2021 International Conference on Data Analytics for Business and Industry, ICDABI 2021, 2021, pp. 118-123, http://dx.doi.org/10.1109/ICDABI53623.2021.9655783

[38] Ha A.C.T., Doumouras B.S., (Nancy) Wang C., Tranmer J., Lee D.S. Prediction of sudden cardiac arrest in the general population: Review of traditional and emerging risk factors Can. J. Cardiol., 38 (4) (2022), pp. 465-478, 10.1016/j.cjca.2022.01.007

[39] Choi Y.A., *et al.* Machine-learning-based elderly stroke monitoring system using electroencephalography vital signals Appl. Sci., 11 (4) (2021),pp. 1-18, 10.3390/app11041761

[40] Prashant Kumar Shrivastava, Mayank Sharma, Pooja sharma, Avenash Kumar, HCBiLSTM: A hybrid model for predicting heart disease using CNN and BiLSTM algorithms, Measurement: Sensors, Vol 25, 2023, 100657, https://doi.org/10.1016/j.measen.2022.100657

Author Biography

Vinoth Rathinam received his Bachelors of Engineering in Electronics and Communication Engineering from Mohamed Sathak Engineering College and Master of Engineering in VLSI Design under Anna University in the years 2007 and 2009, respectively. He received his PhD in Information and Communication Engineering from Anna University in 2017. His area of interest includes Image Processing, Signal Processing and VLSI Design. He has more than 15 years of professional experience in Engineering Colleges. He has received a grant of Rs. 3.5 lakhs for organizing AICTE ATAL FDP during 2023-24. He has been granted 3 patents and has published 16 patents. He has published more than 37 research articles in leading journals and conference proceedings. He is an active reviewer in various peer-reviewed journals of Elsevier, Springer, etc.

Valarmathi K is currently working as a Professor in the Department of Electronics and Communication Engineering at P.S.R. Engineering College, Sivakasi, Tamil Nadu, India. She has 25 years of teaching experience. She has published 46 papers in peer-reviewed international journals and presented 84 papers in various national and international conferences. She has received the best paper award for her paper in the International Conference on VLSI Communication and Instrumentation (ICVCI 2011). Her research interests are System identification, Image processing, soft computing, Wireless networks, Cloud computing and

Manuscript received 30 Dec 2025; Revised 10 Feb 2026; Accepted 20 April 2026; Available online 30 April 2026
Digital Object Identifier (**DOI**): https://doi.org/10.35882/jeeemi.v8i2.1440

Machine Learning. She is the reviewer in various peer-reviewed journals of Elsevier, Springer, Taylor and Francis, IEEE, and Wiley publishers. She has been granted 5 patents and has published 16 patents. She is the recognized supervisor of Anna University, Chennai. 13 PhD scholars have been awarded under her guidance, and 8 scholars are pursuing PhD. She also guided 29 PG Scholars. She received a grant of Rs.70 Lakhs for establishing Process Control and Biomedical Laboratory at Kalasalingam University under DST-FIST scheme, and also received 45 lakhs from AICTE under RPS and MODROB scheme. She delivered many technical talks/lectures in various workshops/seminars on the topic of neural networks, fuzzy logic and soft computing applications. She organized many national/ international level conference/, workshops/seminar and other technical events. She is also a member of the Academic Council, Board of Studies, Department Research Committee and Board of Management in various technical institutions.

Madhumathi. A is currently working as an Assistant Professor in the Department of Electronics and Communication Engineering at P.S.R. Engineering College, Sivakasi, Tamil Nadu, India. She received her Undergraduate degree from PSR Engineering College and her Master of Engineering in Applied Electronics from PSR Engineering College in the years 2023 and 2025, respectively. Her areas of interest include Image Processing, Signal Processing, and Embedded Systems.

Dr. S D Lalitha, working as an Associate Professor in the Department of Computer Science and Engineering, R.M.K. Engineering College, has 25 years of teaching experience. She received her B.E. degree in Computer Science and Engineering from Tagore Engineering College, Chennai and M.Tech degree in Computer Science and Engineering with distinction from Dr. M.G.R Educational and Research Institute, Chennai. She has completed her Ph.D. degree at Anna University, Chennai by 2023. She has published many research papers. Her area of research includes Information and Network Security, Full Stack Development and Artificial Intelligence.

Manuscript received 30 Dec 2025; Revised 10 Feb 2026; Accepted 20 April 2026; Available online 30 April 2026
Digital Object Identifier (**DOI**): https://doi.org/10.35882/jeeemi.v8i2.1440